GRAVITY WAVE DRAG IN A GLOBAL CIRCULATION MODEL OF THE MARTIAN ATMOSPHERE: PARAMETRISATION AND VALIDATION.

M. Collins, S.R. Lewis and P.L. Read

University of Oxford, Atmospheric, Oceanic and Planetary Physics, Clarendon Laboratory, Parks Road, Oxford OX1 3PU, United Kingdom

ABSTRACT

The effect of orographically generated breaking gravity waves is parametrised in a global circulation model of the Martian atmosphere using schemes adapted from terrestrial models. The schemes are 'tuned' by comparing model integrations with and without gravity wave drag with temperatures derived from the Mariner 9 IRIS instrument. Without gravity wave drag the global circulation model temperature field has excessively cold upper level polar regions. Gravity wave drag can correct for such cold temperatures by warming the atmosphere adiabatically via a dynamically induced circulation. The model climatology is significantly improved in the polar regions with the introduction of the parametrisation.

INTRODUCTION

There have been several observational studies of the Martian middle atmosphere that have indicated that, during certain seasons, the polar regions are warmer than expected on the basis of radiative equilibrium (Deming et al., 1986, Théodore et al., 1993, Martin and Kieffer, 1979, Jakosky and Martin, 1987, Santee and Crisp, 1993). As an example we show, in figure 1, the 2am and 2pm temperature fields derived by Santee and Crisp (1993) from the Mariner 9 IRIS instrument at $L_s = 343°$ to $L_s = 348°$ (data kindly supplied by Michelle Santee). There is an inversion of temperature at both 2am and 2pm polewards of 60N as well as a slight indication of a reversed equator to pole temperature gradient (i.e. temperatures increasing towards the pole) in middle latitudes above 40 km. In a similar vein the Viking IRTM $15\mu m$ temperatures showed a marked reversal in horizontal temperature gradient during the 1977b dust storm (Martin and Kieffer, 1979, Jakosky and Martin, 1987).

It is generally accepted that this warming is due to some dynamical phenomena. Consider the theory of the Transformed Eulerian Mean (TEM) Circulation (see e.g. Andrews et al. (1987) page 127). If there is a downward residual mean circulation over the polar regions the atmosphere will be warmed adiabatically above radiative equilibrium. Such downward motion could be the result of a zonal mean circulation or it could be forced by irreversible deformations of the zonally asymmetric flow (eddies). Haberle et al. (1993) have suggested that downward motion over the pole could be caused by the extension of the Hadley Cell to high latitudes during times of high dust. Hollingsworth and Barnes (1996) have suggested the vertically propagating planetary waves could drive a TEM circulation and force downward residual motion over the pole. Finally it has been suggested by Barnes (1990), Théodore et al. (1993) and Joshi et al. (1995) that small scale vertically propagating gravity waves may provide a large enough force on the zonal mean flow to produce a significant warming.

In this paper we concentrate on the latter of these mechanism: gravity wave drag. In particular we focus on orographically generated gravity waves i.e. waves generated via vertical displacements of fluid that occur when the atmosphere blows over a mountain. Under certain conditions these waves can propagate vertically. As they propagate their amplitude increases as the inverse square of the density and at some altitude their amplitude can become so large that potential temperature surfaces become vertical and convective

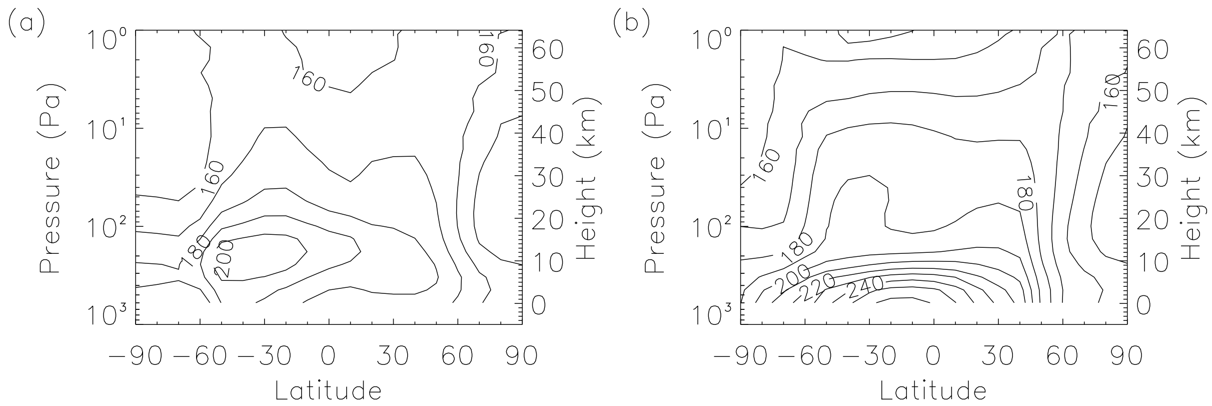

Fig. 1. Temperatures at (a) 2am and (b) 2pm local time retrieved by Santee and Crisp (1993) from the IRIS instrument aboard the Mariner 9 mission. The contour interval is 10K.

overturning creates regions of turbulence. Such turbulence can exert a force on the flow and this force is referred to as gravity wave drag. In general stationary orographic gravity waves exert a retarding force on the mean flow.

In previous work, parameterisations of gravity wave drag have been introduced in to models of the Martian atmosphere of varying complexity. Barnes (1990) adapted the one dimensional quasi-geostrophic model of Holton (1983) for Mars. He found that gravity wave drag, in the form of the Lindzen parametrisation scheme (Lindzen, 1981) was large enough to 'close off' the mid-latitude westerly jet and produce an adiabatic warming of several tens of degrees K. Théodore et al. (1993), motivated by ground based observations of anomalously warm polar temperatures, introduced the Lindzen scheme into a two-dimensional zonally symmetric model of the Martian atmosphere and found, as in Barnes (1990), that gravity wave drag was sufficient to close off the winter jet and produce a significant warming. They also attempted to tune the scheme by comparing observations of eddy diffusion coefficients with those derived from the parametrisation scheme with some limited success. Finally Joshi et al. (1995) have introduce the Lindzen parametrisation into a three dimensional spherical primitive equation model with simplified parametrisations of heating and friction. They concluded, as in the two previous studies, that gravity wave drag could be strong enough to close off the jet and produce a warming. They also noted though that some deceleration of the jet was caused by breaking planetary waves (planetary waves were absent in the studies of Barnes (1990) and Théodore et al. (1993)) which complicates the assessment of the effects of gravity wave drag considerably.

PARAMETRISATION OF GRAVITY WAVE DRAG

For comparison we have taken two gravity wave drag schemes from terrestrial GCMs, the Palmer et al. (1986) scheme and the Lott and Miller (1996) scheme, and adapted them for Martian conditions. Both schemes represent the effects of an ensemble of gravity waves by parametrising just one stationary gravity wave but including some tunable parameter to account for the other waves. Spectral schemes (e.g. Hines, 1996, Fritts and Lu, 1993) have recently emerged but are computationally very expensive and have yet to be implemented even in state-of-the-art terrestrial models.

Full details of both schemes are given in Lott and Miller (1996), Miller et al. (1989), Baines and Palmer (1990) and Palmer et al. (1986) but we give a brief description here. We represent the surface stress, τ induced by a single orographically generated gravity by one of two expressions. Either (Palmer et al., 1986)

$$\tau = \kappa \rho N u \mu^2 \tag{1}$$

where ρ is the density, N the Brunt-Viäsälä frequency, $\mathbf{u}$ the low level wind (vertically averaged in the lowest 3 model levels in our case), μ^2 the vector sub-grid scale orographic variance and κ can be thought of as the wavenumber of the gravity wave or as a legitimately tunable parameter. Or we use (Baines and Palmer, 1990, Lott and Miller, 1996)

$$\tau = \rho U N \mu \sigma G (B \cos^2 \psi + C \sin^2 \psi, (B - C) \sin \psi \cos \psi). \tag{2}$$

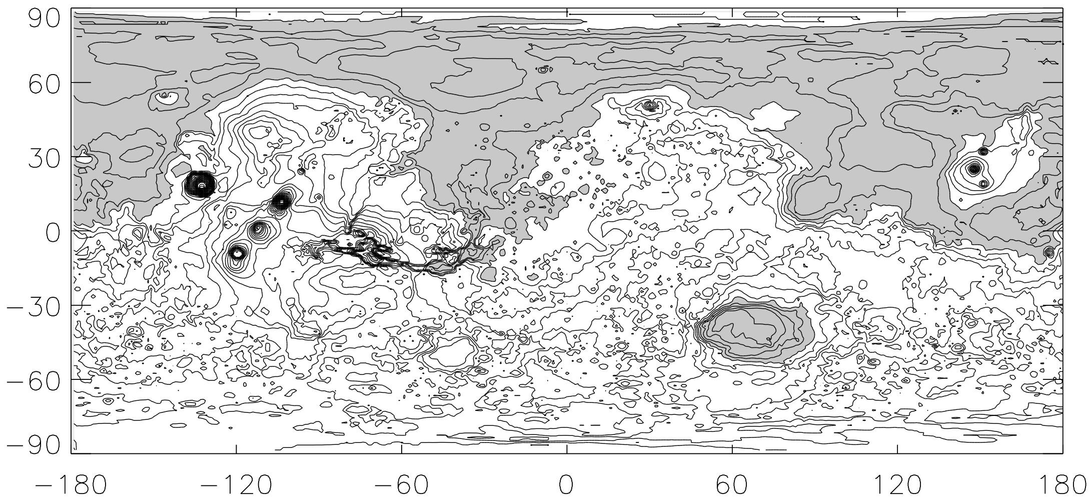

Fig. 2. The DTM orography at $\frac{1}{4}^\circ \times \frac{1}{4}^\circ$ resolution relative to the zero datum. The contour interval is 1 km and areas below the zero datum are shaded.

where $U = |\mathbf{u}|$, G is a constant of order unity, $B = 1 - 0.18\gamma - 0.04\gamma^2$, $C = 0.48\gamma + 0.3\gamma^2$ and σ, μ, γ and ψ are the sub-grid scale orographic slope, standard deviation , anisotropy and angle between the mean wind a the principal axes of the orography respectively. The reader is referred to Baines and Palmer (1990) and Lott and Miller (1996) for definitions of these parameters. Also, as in Lott and Miller (1996) we represent the effects of form drag which occurs when the low level flow is blocked by the mountain.

Once the surface stress is known, the gravity wave is propagated vertically through the atmosphere with its amplitude adjusted according to the density profile. We judge the effect of the wave on the mean flow by calculating the minimum Richardson number (Ri_{min}) attainable i.e. the Richardson number that is 'felt by the gravity wave' and employ the saturation hypothesis of Lindzen (1981). If Ri_{min} drops below a critical value (Ri_c) the gravity wave amplitude is re-evaluated in order to keep $Ri_{min} = Ri_c$. This gives a vertical profile of momentum flux from which we calculate the wind tendency by taking the vertical derivative.

Sub-Grid Scale Orography

The sub-grid scale orographic parameters σ, μ, γ and ψ have been calculated from the Digital Topographic Model (DTM) orography (Wu, 1981) at a resolution of $\frac{1}{4}^\circ \times \frac{1}{4}^\circ$. This is shown in figure 2. The DTM was derived from stereo photography techniques during the Viking mission and although it may be suspect on large scales (the Viking lander sites are at the wrong relative heights) it is believed that the small scale features, that may be responsible for the generation of gravity waves, are well represented. The alternative orographic data set is the Consortium orography which is very smooth on small scales and is of little use. Note in figure 2 the large amount of cratering in the southern hemisphere which may be important in the generation of gravity waves.

The most important sub-grid scale parameter in both the formulations of surface stress (equations 1 and 2) is likely to be the orographic standard deviations μ. This is shown in figure 3 smoothed to T21 resolution (see the next section) for which all the model experiments were run. The largest contribution to the standard deviation comes from the shield volcanoes that sit atop the Tharsis plateau. Elsewhere μ is on the order of 1000m which is consistent with there being small scale features in figure 2 that are picked out with a contour interval of 1000m. Note that μ is, in general, larger in the southern hemisphere than in the northern hemisphere (because of the large number of craters there). All other things being equal one will expect gravity wave activity to be greater in the southern hemisphere compared to the north.

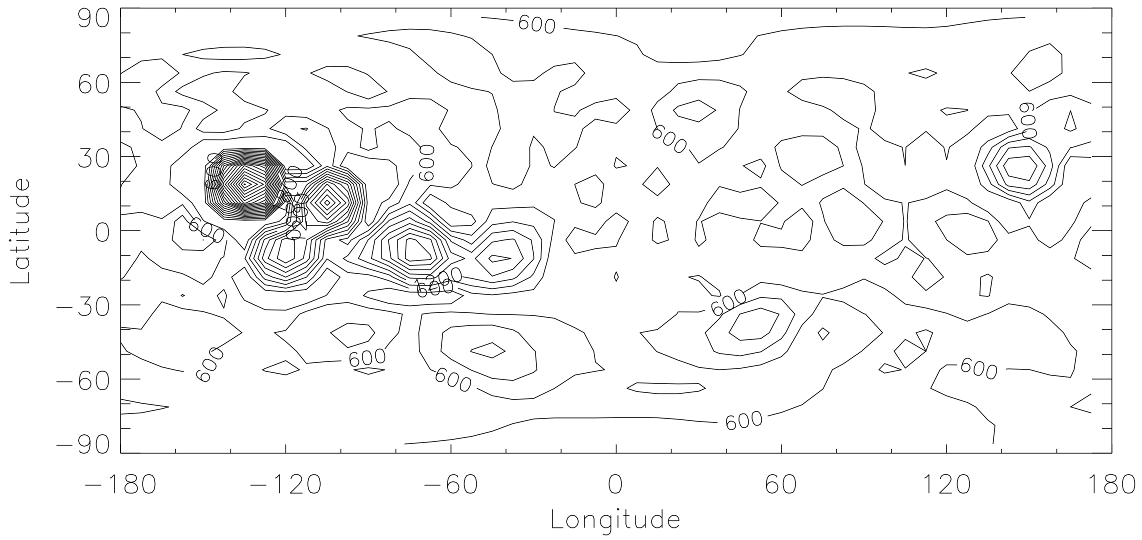

Fig. 3. The sub-grid scale orographic standard deviation at T21 resolution defined from the DTM shown in figure 2. The contour interval is 300m.

THE GLOBAL CIRCULATION MODEL

We have implemented the gravity wave drag scheme in the Oxford Martian Global Circulation Model (MGCM). The model and it's climatology are described in Read et al. (1996) and elsewhere (Collins et al., 1994, Collins et al., 1996). Briefly the model solves the primitive equations of meteorology using the spectral method of Hoskins and Simmons (1975) in the horizontal and finite differencing in the vertical. It contains a host of parametrisation schemes relevant to the Martian atmosphere developed at the Laboratoire de Météorologie Dynamique (Hourdin, 1992, Hourdin et al., 1993, Hourdin et al., 1995). Each of our experiments are carried out at a spectral resolution of total wavenumber 21 and with 20 levels in the vertical ranging from an altitude of approximately 80 m at the surface to approximately 80 km at the top of the model.

VALIDATION

Control Integration: No Gravity Wave Drag

We first set the dust distribution to that given by Santee and Crisp (1993), having a vertical distribution of dust absorption coefficient,

$$k(p) \;=\; k_s \exp\left(0.01\left(1-\frac{p_s}{p}\right)\right) \tag{3}$$

where p is the pressure, p_s the surface pressure and k_s can be found by integrating

$$\tau_d \;=\; \int_0^{p_s} k_s \exp\left(0.01\left(1-\frac{p_s}{p}\right)\right) dp \tag{4}$$

where τ_d is the column-integrated dust optical depth. The horizontal distribution was set using an 8^{th} order polynomial fit to figure 9 of Santee and Crisp (1993). This is shown in figure 4.

In the first instance the model was run out to day 600 ($L_s = 323°$) with no gravity wave drag scheme. The model state at day 600 was then used as the initial condition for all the subsequent sensitivity experiments. Each experiment was run out until day 647.6 ($L_s = 348°$) and the model history was sampled 5 times a day for the last 10 days of this run to correspond with the period covered by the retrievals of Santee and Crisp (1993) ($L_s = 343°$ to $L_s = 348°$).

Figure 5 shows the 2am and 2pm temperatures from the control run (no gravity wave drag scheme) as well as the difference between these fields and the retrievals shown in figure 1. There are large differences (greater

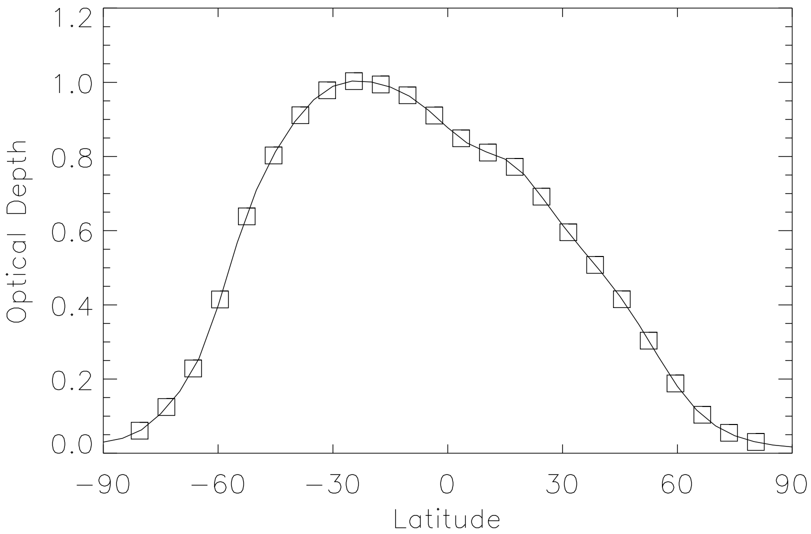

Fig. 4. Visible column dust optical depth from Santee and Crisp (1993). Squares show the retrieved dust and the solid line shows an 8th order polynomial fit to those values.

than 30K in some regions) between the model and the retrievals. In particular we note that in both the southern and northern polar regions at upper levels the model is colder than the retrievals. This is precisely the sort of error that is probably due to the lack of gravity wave drag in the model (although errors in the mean circulation or resolved eddies cannot be ruled out). Differences between the model and the retrievals in equatorial regions are almost certainly due the fact that the retrieved temperatures are statically unstable in this region. The model has a dry convective adjustment scheme that adjust the temperatures to neutral whenever instability occurs so we cannot hope for a good fit near the equator.

The first thing to note is that there is some warming above radiative equilibrium at upper levels in the polar regions even in the absence of gravity wave drag. This is due to a deceleration of the westerlies at upper levels via resolved gravity and planetary wave breaking. Figure 6(a) shows the zonal mean zonal wind for this simulation. Note the region of reversed shear in the southern hemisphere at upper levels and the region of reduced shear at upper levels in the northern hemisphere.

Impact of the Sub-grid Scale Orographic Scheme

Now we asses the impact of the gravity wave drag scheme. The model was run out from day 600 with the Palmer et al. (1986) scheme implemented and the results sampled as before. The tunable parameter, κ, was set at $1.5 \times 10^{-5}\ m^{-1}$ corresponding to a gravity wave with a horizontal wavelength of the order of the grid-scale. Figure 7 shows the 2am and 2pm temperature fields as well as the differences from the retrievals for this run. In the equatorial regions and in middle latitudes the scheme has had little impact, while in the polar regions at upper levels the temperatures are now markedly warmer than the retrievals. This indicates that the gravity wave drag is too strong. The effect of the scheme on the zonal mean zonal wind can be seen in figure 6(b). The strength of the mid-latitude westerly jets have been severely reduced by the drag.

Figure 8 shows the impact of the gravity wave drag on the model in terms of the temperature change it can induce. The scheme can only change the temperature at upper levels in the polar regions as this is where the zonal flow is affected by the gravity wave drag (the temperature structure is altered via dynamical balance - see the introduction). Hence we can only expect to fit the temperature in these regions.

Best Fit Case: Palmer et al. Scheme

The best fit between the model and the retrievals was picked from over 20 sensitivity cases and is achieved with $\kappa = 3 \times 10^{-7}$. Figure 9 shows again the 2am and 2pm temperatures and error fields for this simulation. The error field is as low as 10K at upper levels in both polar regions which is within the retrieval error of the observations. The drag is in fact rather small in this simulation. This can be seen from the zonal mean

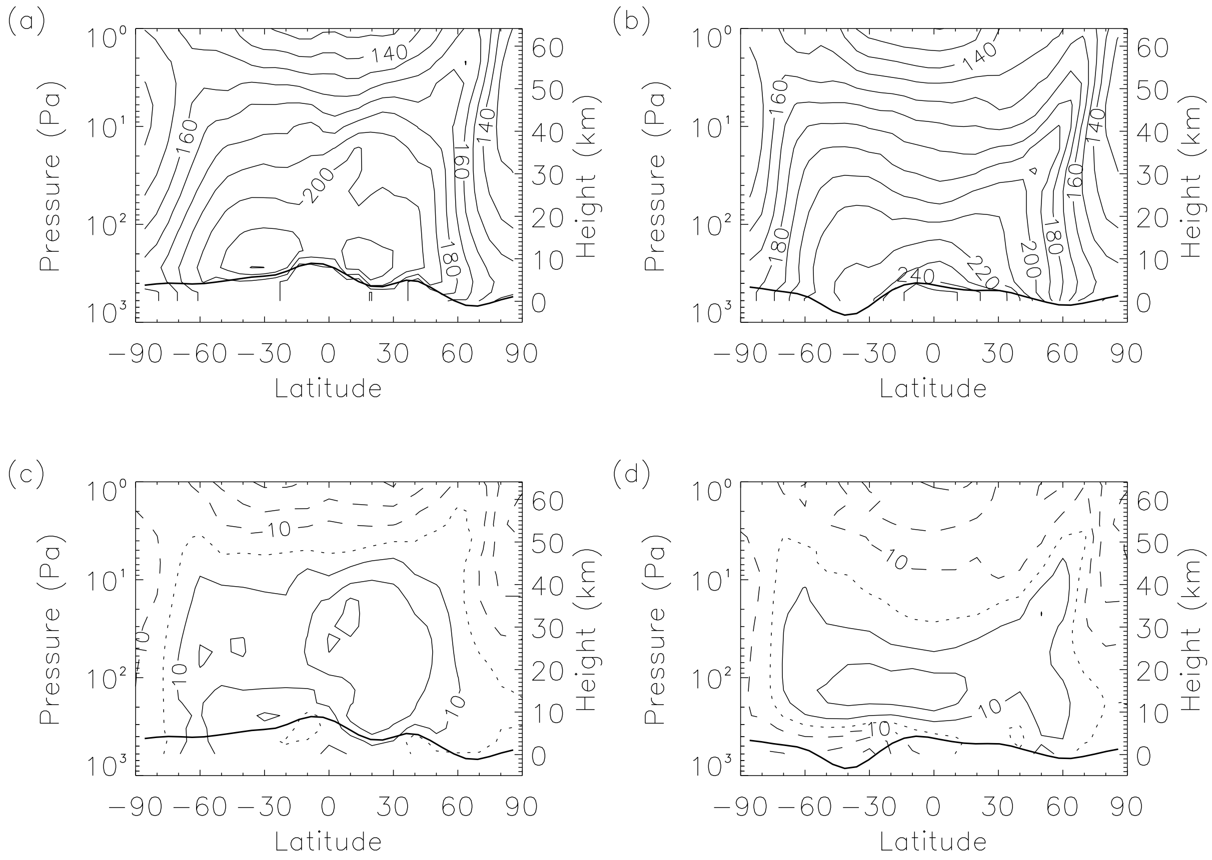

Fig. 5. Model temperatures from the integration with no gravity wave drag scheme. (a) 2am temperature, (b) 2pm temperature, (c) difference between the model and the retrievals at 2am, (d) difference between the model and the retrievals at 2pm. Solid contours indicate positive values, dashed contours negative and the zero contour is dotted. The contour interval is 10K in each plot. The thick black line represents the model orography.

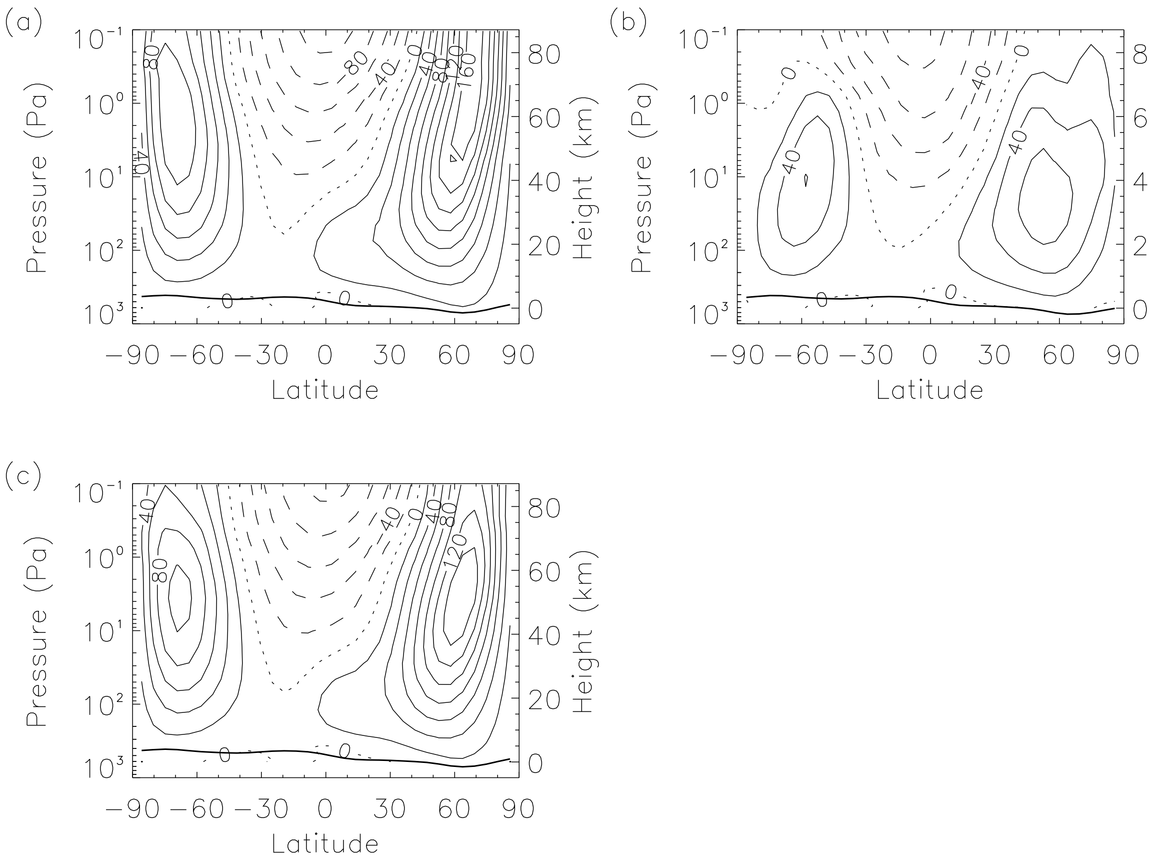

Fig. 6. Zonally averaged zonal wind from (a) the integration with no gravity wave drag scheme, (b) the integration with gravity wave drag and the first guess parameters, and (c) the integration with the best fit parameters. Solid contours indicate positive values, dashed contours negative and the zero contour is dotted. The contour interval is 20 m s^{-1} in each plot. The thick black line represents the model orography.

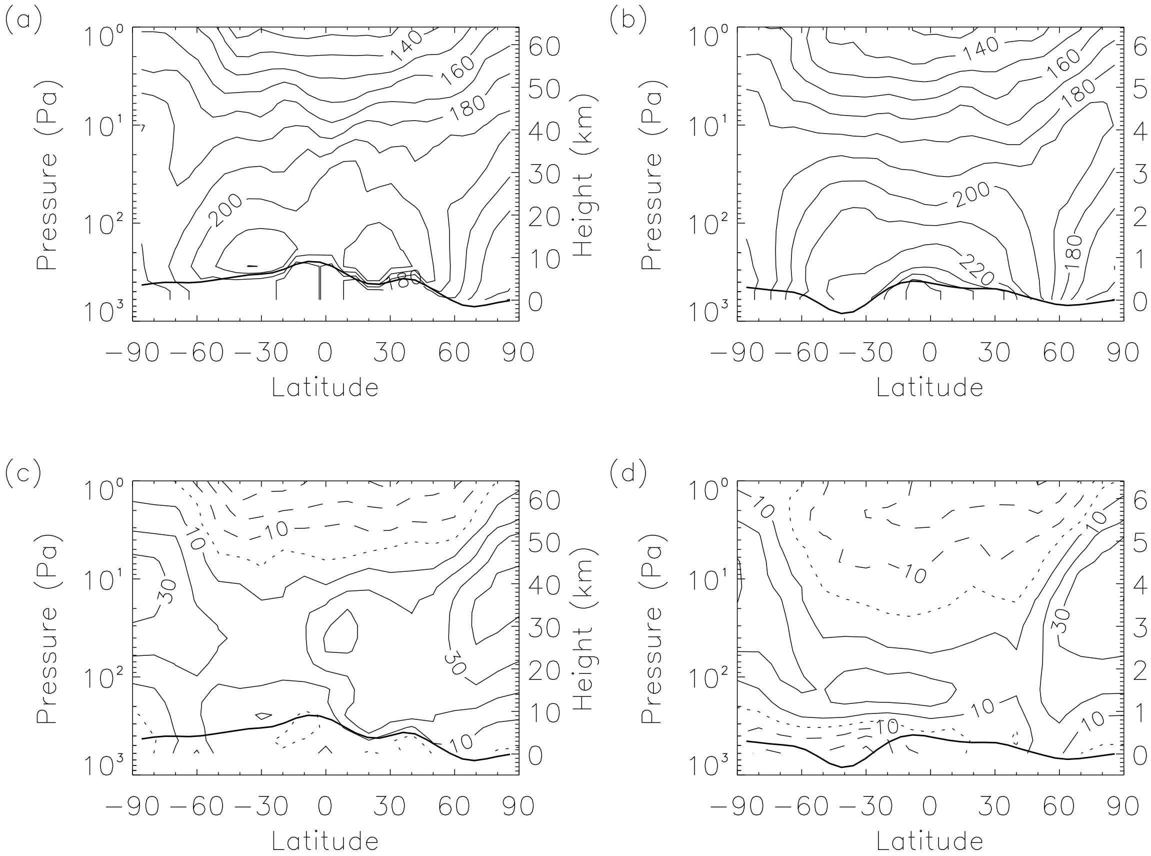

Fig. 7. Model temperatures from the integration with the first guess gravity wave drag scheme. (a) 2am temperature, (b) 2pm temperature, (c) difference between the model and the retrievals at 2am, (d) difference between the model and the retrievals at 2pm. Solid contours indicate positive values, dashed contours negative and the zero contour is dotted. The contour interval is 10K in each plot. The thick black line represents the model orography.

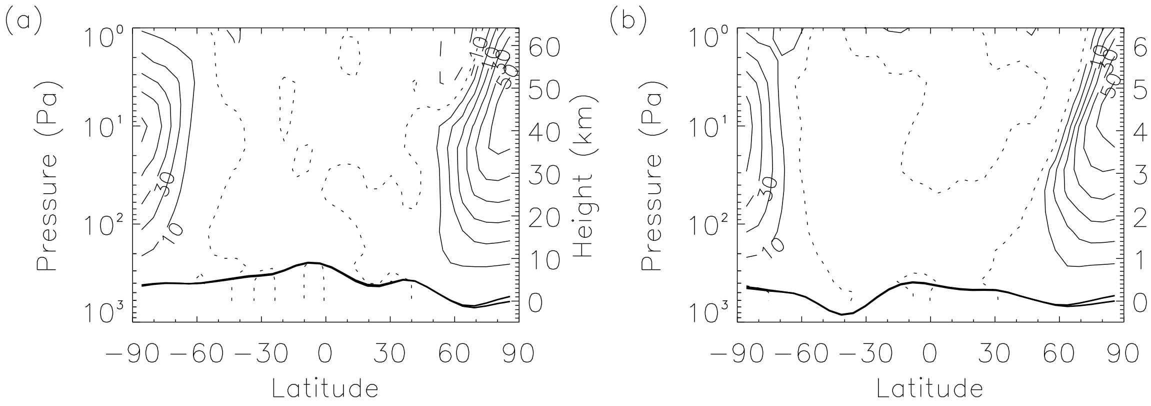

Fig. 8. Temperature difference between the model run with the gravity wave drag scheme and without the gravity wave drag scheme at (a) 2am, and (b) 2pm. Gravity wave drag causes a warming at upper levels in the polar regions but does not affect the temperature elsewhere. Solid contours indicate positive values, dashed contours negative and the zero contour is dotted. The contour interval is 10K in each plot. The thick black line represents the model orography.

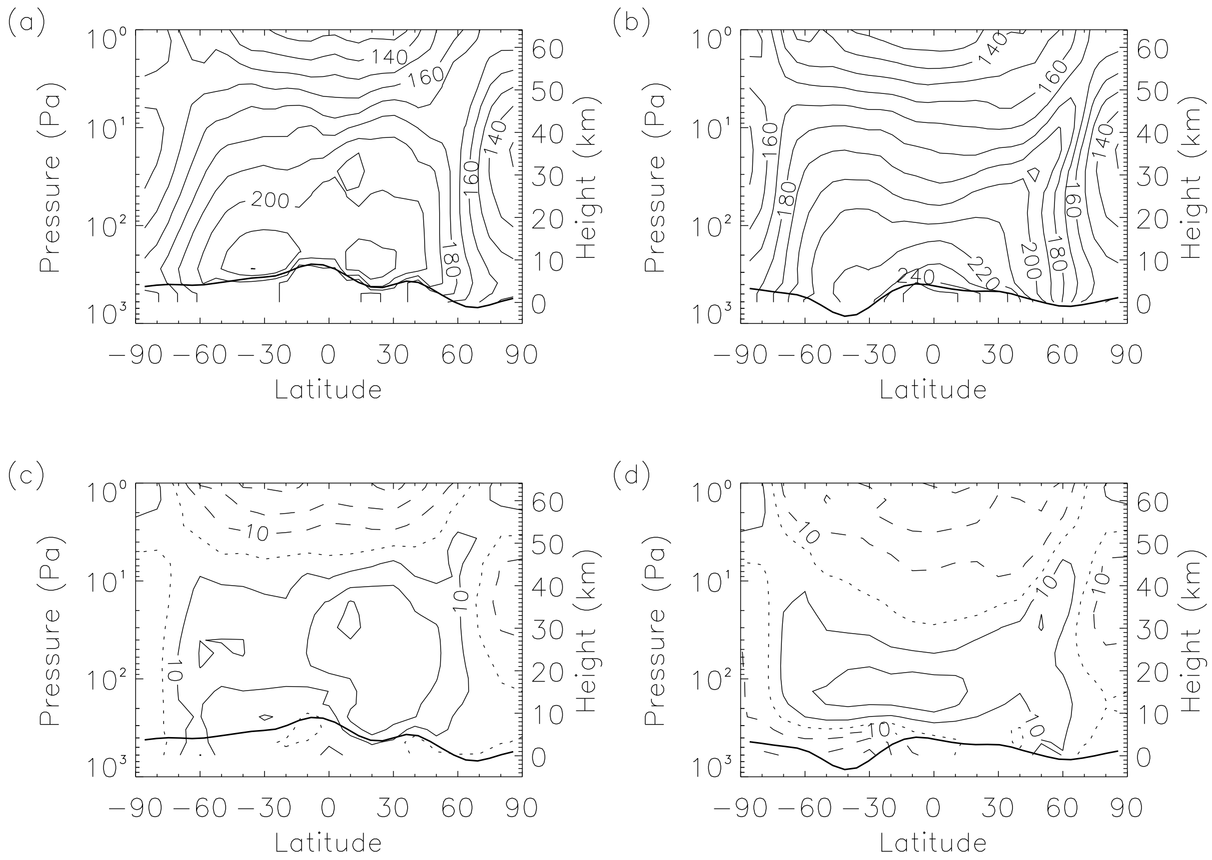

Fig. 9. Model temperatures from the best fit integration using the Palmer et al. scheme. (a) 2am temperature, (b) 2pm temperature, (c) difference between the model and the retrievals at 2am, (d) difference between the model and the retrievals at 2pm. Solid contours indicate positive values, dashed contours negative and the zero contour is dotted. The contour interval is 10K in each plot. The thick black line represents the model orography.

zonal wind in figure 6(c). The mid-latitude westerlies have not been reduced greatly compared with the case without gravity wave drag (figure 6(a)).

We must note though that this fit is in no way optimal. There are both systematic and random errors in the retrieval of the temperatures and dust amounts, and both systematic and random errors in the model. The 'best fit' value of κ is two orders of magnitude smaller than what would be expected on the basis of theory. Palmer et al. (1986) found reasonable values of the surface stress with a value for κ smaller than suggested by linear theory, but only by a few percent. Bougeault et al. (93) even suggest that κ should be set larger than suggested by linear theory. We should really add some error estimate for κ based on some approximate estimate of the errors in both the retrievals and in the model however there is no clear objective way of doing this.

<u>Best Fit Case: Lott and Miller Scheme</u>

We also performed the validation exercise with the Baines and Palmer (1990) scheme i.e. using eq. 2 and tuning G. The best fit was achieved with $G = 0.1$ and simulation appears to be very similar to that shown in figure 9 for the Palmer et al. (1986) scheme.

CONCLUSIONS

We have introduced two parametrisations of orographic gravity wave drag into a global circulation model of the Martian atmosphere. The schemes have been tuned by comparing the model temperatures with those retrieved by Santee and Crisp (1993) from spectra taken by the IRIS instrument aboard Mariner 9. Without gravity wave drag the model is too cold at upper levels in the polar regions. Gravity wave drag can induce a dynamical warming to 'correct' the model in these regions and produce a more realistic simulation.

It is worthy of note that the optimal parameters for the scheme are somewhat smaller than those expected on the basis of theory. One possible deficiency in the scheme is the lack of radiative damping of gravity waves. Imamura and Ogawa (1995) give radiative damping rates for gravity waves on Mars showing them to be at least an order of magnitude more rapid than those on the Earth. Also the assumption of parametrising only one gravity wave is rather restrictive. The next stage in this research will be to introduce spectral scheme (e.g. Fritts and Lu, 1993, Hines, 1996) into the model.

Finally we must add several caveats to the main conclusions of this paper. There are several sources of error in the model fit we have presented. There are certainly systematic and random errors in the model. In particular the dust distribution, which is a very sensitive parameter in Martian GCMs is poorly known from the IRIS spectra. Also some of the deceleration of the westerly jet and associated polar warming is cause by resolved dynamical processes. If these processes are poorly modelled then the best fit gravity wave drag will be either an over or under compensation for other errors in the model (however we note that gravity wave drag is often used as a kind of 'fudge factor' in terrestrial GCMs). Finally there are almost certainly systematic and random errors in the temperature retrievals (possibly of the order of 10K in some regions) notwithstanding poor spatial and temporal coverage.

Finally we look towards missions like Mars Global Surveyor together with model inter-comparisons (Read et al., 1997) and data assimilation studies (Lewis et al., 1997) to aid in the parametrisation of gravity wave drag in the future.

ACKNOWLEDGEMENTS

We thank Michelle Santee for providing the retrieved IRIS temperatures and Francois Lott for providing his gravity wave drag scheme. This work was supported by the UK Particle Physics and Astronomy Research Council and from ESTEC contract 11369/95/NL/JG(SC).

REFERENCES

Andrews, D. G., J. R. Holton, and C. B. Leovy, *Middle Atmosphere Dynamics.* Academic Press (1987).

Baines, P. G., and T. N. Palmer, Rationale for a new physically-based parametrisation of sub-grid scale orographic effects., Tech. Rep. 169, ECMWF (1990).

Barnes, J. R., Possible effect of breaking gravity waves on the circulation of the middle atmosphere of Mars, *J. Geophys. Res.*, 95, 1401–1421 (1990).

Bougeault et al., P., The atmospheric momentum budget over a major mountain range: first results of the PYREX field program., *Ann. Geophys.*, 11, 395–418 (93).

Collins, M., S. R. Lewis, and P. L. Read, Regular and irregular baroclinic waves in a martian general circulation model: A role for diurnal forcing?, *Adv. Space. Res.*, 16(6), 3–7 (1994).

Collins, M., S. R. Lewis, P. L. Read, and F. Hourdin, Baroclinic wave transitions in the martian atmosphere, *Icarus*, 120, 344–357 (1996).

Deming, D. J., F. Mumma, F. Espenak, T. Kostius, and D. Zipoy, Polar warming in the atmosphere of Mars, *Icarus*, 66, 366–379 (1986).

Fritts, D. C., and W. Lu, Spectral estimates of gravity wave energy and momentum fluxes. part ii: Parameterization of wave forcing and variability., *J. Atmos. Sci.*, 50, 3093–3124 (1993).

Haberle, R. M., J. B. Pollack, J. R. Barnes, R. W. Zurek, C. B. Leovy, J. R. Murphy, H. Lee, and J. Schaeffer, Mars atmospheric dynamics as simulated by the NASA/Ames general circulation model I. The zonal-mean circulation, *J. Geophys. Res.*, 98(E2), 3093–3124 (1993).

Hines, C. O., Doppler-spread parametrisation of gravity-wave momentum depostion in the middle atmosphere. part 1: Basic formulation., *Submitted to J. Atm. Terr. Phys* (1996).

Hollingsworth, J. L., and J. R. Barnes, Forced, stationary planetary waves in Mars' winter atmosphere., *J. Atmos. Sci.* (1996).

Holton, J. R., The influence of gravity wave breaking on the general circulation of the middle atmosphere., *J. Atmos. Sci.*, 40, 791–799 (1983).

Hoskins, B. J., and A. J. Simmons, A multi-layer spectral model and the semi-implicit method, *Q. J. R. Meteorol. Soc.*, 101, 637–655 (1975).

Hourdin, F., A new representation of the CO_2 15μm band for a Martian general circulation model, *J. Geophys. Res.*, 97(E11), 18,319–18,335 (1992).

Hourdin, F., P. Le Van, F. Forget, and O. Talagrand, Meteorological variability and the annual surface pressure cycle on Mars, *J. Atmos. Sci.*, 50, 3625–3640 (1993).

Hourdin, F., F. Forget, and O. Talagrand., The sensitivity of the Martian surface pressure to various parameters: a comparison between numerical simulations and Viking observations, *J. Geophys. Res.*, 100, 5501–5523 (1995).

Imamura, T., and T. Ogawa, Radiative damping of gravity waves in the terrestrial planetary atmospheres, *Gephys. Res. Letts.*, 22(3), 267–270 (1995).

Jakosky, B. M., and T. Z. Martin, Mars: North-polar atmospheric warming during dust storms, *Icarus*, 72, 528–534 (1987).

Joshi, M. M., B. N. Lawrence, and S. R. Lewis, Gravity wave drag in three-dimension atmospheric models of Mars, *J. Geophys. Res.*, 100, 21235–21245 (1995).

Lewis, S. R., M. Collins, and P. L. R. Read, Data assimilation with a martian global circulation model, *Adv. Space Res.*, This Issue (1997).

Lindzen, R. S., Turbulence and stress owing to gravity wave and tidal breakdown, *J. Geophys. Res.*, 86, 9707–9714 (1981).

Lott, F., and M. Miller, A new sub-grid scale orographic drag parametrization: its formulation and testing., *Q. J. R. Meteorol. Soc.*, In Press (1996).

Martin, T. Z., and H. H. Kieffer, Thermal infrared properties of the Martian atmosphere, 2, the 15μm band measurements, *J. Geophys. Res.*, 84(B6), 2843–2852 (1979).

Miller, M. J., P. M. Palmer, and R. Swinbank, Parametrisation and influence of sub-grid scale orography in general circulation and numerical weather prediction models., *Meteor. & Atmos. Phys.*, 40, 84–109 (1989).

Palmer, T. N., G. J. Shutts, and R. Swinbank, Alleviation of a systematic westerly bias in general circulation and numerical weather prediction models through an orographic gravity wave drag parametrisation, *Q. J. R. Meteorol. Soc.*, 112, 1001–1039 (1986).

Read, P. L., M. Collins, and S. R. Lewis, The Oxford Mars global circulation model: Formulation and climatology, *In preparation*, Pre-prints available on request (1996).

Read, P. L., M. Collins, S. R. Lewis, F. W. Taylor, F. Hourdin, F. Forget, and O. Talagrand, A GCM climate database for the Mars, for sicence and mission planning, *Adv. Space Res.*, This Issue (1997).

Santee, M., and D. Crisp, Thermal structure and dust loading of the Martian atmosphere during late southern summer: Mariner 9 revisited, *J. Geophys. Res.*, 98, 3261–3279 (1993).

Théodore, B., E. Lellouch, E. Chassefiere, and A. Hauchecorne, Solsticial temperature inversions in the Martian middle atmosphere : observational clues and 2-D modeling, *Icarus*, 105, 512–528 (1993).

Wu, S. S. C., A method of defining topographic datums of planetary bodies, *Annales de Geophysique*, 1, 147–160 (1981).